

# Granular fingers in Hele-Shaw experiments

M.S. Couto, M.L. Martins & S.G. Alves  
Departamento de Física, Universidade Federal de Viçosa,  
36571-000, Viçosa, MG, Brazil

*PACS numbers:* 47.54.+r, 45.70.-n, 45.70.Mg, 45.70.Qj

*Key-words:* granular materials, Hele-Shaw, pattern formation

Granular materials constitute an intermediate state of matter between fluids and solids[1]. Over the past decade, a large series of experimental assays on granular systems, concentrated in the quantitative studies of compaction, mixing, segregation and patterns formed by vibration, have been done[2-9]. They uncovered numerous mechanisms (percolation, convection, ordered settling, arching, etc.) for segregation of dissimilar grains; remarkable standing-wave patterns (stripes, hexagons, disordered waves, cluster of localized solitary excitations, etc.) in vibrating layers of granular materials and highly inhomogeneous and localized stresses chains in nearly static granular media. Nevertheless, in contrast to viscous fingering in fluids, a widely studied pattern-forming phenomena[9], grain-grain displacement seems to be an unexplored area in granular physics. Here we investigate the pattern formation when a grain is displaced by another type of grain in a radial Hele-Shaw cell. We show that several morphologies can occur, ranging from rounded to fingered patterns, interconnected by a continuous crossover. Fourier analyses shows that, in contrast to the rounded patterns, the fingered shapes present mode selection.

The experiments were carried out in a radial Hele-Shaw cell made of two parallel square glass plates, each with a thickness of 0.5 cm and lengths of 90 cm (bottom plate) and 80 cm (top plate). The top plate had a hole of 0.5 cm in diameter in its centre for the injection of grains. Initially, a dense uniform circular monolayer of styrofoam spheres was formed on the cell's bottom plate, always covering the same area. After that, the cell was closed with the top plate, over which weights were placed to prevent upward movement, and another kind of grain was injected through its hole. In all experiments steel spheres with a diameter of  $3.94 \pm 0.03$  mm were manually injected, whereas three types of styrofoam initial monolayers were used: type *A*, with an average diameter of  $2.3 \pm 0.1$  mm and low polydispersion; type *B*, composed of spheres with diameters in the range of 0.5 to 4.0 mm and average diameter of  $2.9 \pm 0.6$  mm; and type *C*, with an average diameter of  $3.5 \pm 0.3$  mm and low polydispersion. After

every 100 g of injected spheres, corresponding to the mass of  $N = 395$  spheres, the growing patterns were photographed in order to follow their evolution.

Different displacement patterns were observed as a function of the diameters of the styrofoam spheres and the plates separation. In Fig. 1, a pattern  $\sim 50$  cm wide showing well developed fingers, formed after the injection of 6715 steel spheres can be seen. In addition to the expected interface between the steel/styrofoam spheres, there is an additional interface in the displaced grains. This second interface is the border between two regions: an outer one, still a dense monolayer, and an inner one in which the spheres have moved upward and, hence, is no longer a monolayer. All the displacement patterns generated in the experiments exhibited this second interface. Also present is a similar upward movement of the displacing steel spheres.

In Fig. 2, a qualitative morphological diagram is proposed based on the data available from the limited range of grains diameters and plates separations  $D$  tested in our experiments. For large  $D$  ( $> 5.60$  mm) the displacement patterns are circular. For intermediate  $D$  (ranging from 5.17 to 5.60 mm), the interface of injected steel spheres exhibit small wavy or cusp instabilities for type *A* (small) or type *B* (intermediate) displaced styrofoam spheres, respectively. For small  $D$  ( $< 5.17$  mm) fingered patterns are observed, including fingers having pronounced tip splitting, resembling the branched erosion channels formed in water/glycerine saturated Fointanebleau sand[10], for the smallest  $D$ . For a given value of  $D$ , the fingers become more apparent as the average diameter of the displaced styrofoam spheres is increased. All, these different morphological phases are probably not separated by sharp phase transitions and, instead, continuous crossovers among them might be observed. Indeed, in Fig. 3, the patterns formed by the steel spheres in styrofoam spheres of type *B*, suggest a continuous crossover from a fingered pattern (Fig. 3a) to an almost circular one (Fig. 3d), as the plates separation  $D$  increases. The number of injected spheres ( $N = 6320$ ) and the scale of the drawings are the same for all patterns showed in Fig. 3. From now on, the sequence of patterns observed in Fig. 3, which represents a cut of constant average diameter (type *B*) in the morphological diagram will be analysed. Similar behaviours are found for other parallel cuts.

From Fig. 4, in which the distance of each point along the border to the mass centre of the pattern is represented, one can see the time evolution of the patterns depicted in Fig. 3a,d. For the fingered pattern, the formation and splitting of the fingers can be clearly seen (Fig. 4a-c). On the contrary, for the rounded pattern, although its average radius increases in time, the deviation around this value remains small, and fingers are not formed (Fig. 4d-f). Figure 5 shows the Fourier transforms of the displacement borders in Fig. 4. For the fingered pattern of Fig. 3a, it is possible to see that, as its size increases and the fingers become more pronounced, modes are selected, which shift from high to low wave numbers (Fig. 5a-c). Rauseo et al.[11] have observed the same behaviour for the power spectra of the curvature versus arc length along the interface of the patterns generated by fluid-fluid displacement for their regime of fast flows. Conversely, for the pattern of Fig. 3d, which remains rounded during the growth, no mode selection is observed (Fig. 5d-f).

In fluid-fluid displacement the fingers are formed when a low viscosity fluid is injected in a high viscosity one. For the systems studied here, we suspect that the role of viscosity is played by the friction of the grains against themselves and the plates of the cell. The great elasticity of the styrofoam spheres enhances this friction since they can deform and increase their contact area, providing a higher “effective viscosity” as compared to the one for the steel spheres. This increase in friction becomes more critical as the plates separation is decreased, leading to more pronounced fingers in the formed patterns. In fact, experiments in which the styrofoam spheres were replaced by hard plastic beads generated less conspicuous fingers as compared to the ones formed in styrofoam for the same plates separation. The relationship between friction and “effective viscosity” can explain why finger instability occurs only after a certain number of steel spheres have been injected. At the beginning, the resistance against the displacement front is small since the styrofoam spheres, apart from some isolated defects, initially form a monolayer. Consequently, its “effective viscosity” is low (comparable to that for the steel spheres), and the border of the displacement pattern is circular with small fluctuations superimposed. As the injection proceeds, the styrofoam spheres pile up and can jam in a crescent number of points, increasing their “effective viscosity”. When this value overcomes the “viscosity” of the driving grains, the circular interface becomes unstable and fingers begin to form. Since the stress generated by the injected grains concentrates at the finger tips, the jammed styrofoam spheres in these regions are eventually released due to their elasticity, leading to a fast growth of the fingers. In contrast, if hard plastic beads, which can be deformed only slightly, are used, the stress concentration at the fingers is not sufficient to loose the jammed beads around them, consequently, slowing down the tip growth and contributing to stabilise a circular displacement front.

The width of the multilayered region depends on the plates separation. For large separations the styrofoam spheres can easily move upward, releasing the stress caused by the displacing grain in a narrow region. On the contrary, for small separations the upward movement of the styrofoam is hindered and a wider region is necessary to release the stress. As the pattern develops, the driving front faces an increasing resistance, directly observed by the crescent force necessary to inject the steel spheres in the cell. At later stages of the experiment, even the displacing grains are under a so large stress that the steel spheres themselves begin to move upward, initially in a region close to the injection point and then spreading across the pattern. Differently than for the styrofoam spheres, even for the largest plates separation used, the steel spheres cannot rise enough to form a bilayer. The multilayered region in the styrofoam, as well as in the steel spheres, never reaches the outermost ones. There is always a monolayer of spheres that seems to be free of stress.

The main result of this experimental study was the discovery that several morphologies, connected by a continuous crossover, can be found for grain-grain displacement in a radial Hele-Shaw cell. It was possible to observe that the formation of fingered patterns proceeds through the selection and amplification of characteristic wavelengths. We are currently refining

the morphological diagram and investigating the complex stress distribution in this granular system. In particular, the effects of elasticity will be the focus of the next experiments.

## References

- [1] Jager, H.M., Nagel, S.R. & Behinger, R.P. Granular solids, liquids, and gases. *Rev. Mod. Phys.* **68**, 1259-1273 (1996).
- [2] Mueth, D.M. et al. Signatures of granular microstructure in dense shear flows. *Nature* **406**, 385-389 (2000).
- [3] Villarruel, F.X., Lauderdale, B.E., Mueth, D.M. & Jaeger, H.M. Compaction of rods: relaxation and ordering in vibrated, anisotropic granular material. Pre-print cond-mat/0001457 at <<http://xxx.lanl.gov>> (01 February 2000).
- [4] Sinbrot, T. & Muzzio, F.J. Nonequilibrium patterns in granular mixing and segregation. *Phys. Today* **53**(3), 25-30 (2000) and references therein.
- [5] Melo, F., Umbanhowar, P.B. & Swinney, H.L. Transition to parametric wave patterns in a vertically oscillated granular layer. *Phys. Rev. Lett.* **72**, 172-175 (1994).
- [6] Melo, F., Umbanhowar, P.B. & Swinney, H.L. Hexagons, kinks, and disorder in oscillated layers. *Phys. Rev. Lett.* **75**, 3838-3841 (1995).
- [7] Metcalf, T.H., Knight, J.B. & Jaeger, H.M. Standing wave patterns in shallow beds of vibrated granular material. *Physica A* **236**, 202-210 (1997).
- [8] Umbanhowar, P.B., Melo, F. & Swinney, H.L. Localized excitations in a vertically vibrated granular layer. *Nature* **382**, 793-796 (1996).
- [9] Meakin, P. *Fractals, Scaling and Growth far from Equilibrium* (Cambridge University Press, Cambridge, 1998).
- [10] Mills, P., Cerasi, P. & Fautrat, S. Erosion instability in a non-consolidated porous-medium. *Europhys. Lett.* **29**, 215-220 (1995).
- [11] Rauseo, S.N., Barnes, Jr., P.D. & Maher, J.V. Development of radial fingering patterns. *Phys. Rev. A* **35**, 1245-1251 (1987).

M.L. Martins is funded by CNPq, Brazilian Agency.

Correspondence and requests for materials should be addressed to M.S. Couto (e-mail: [mscouto@mail.ufv.br](mailto:mscouto@mail.ufv.br)).

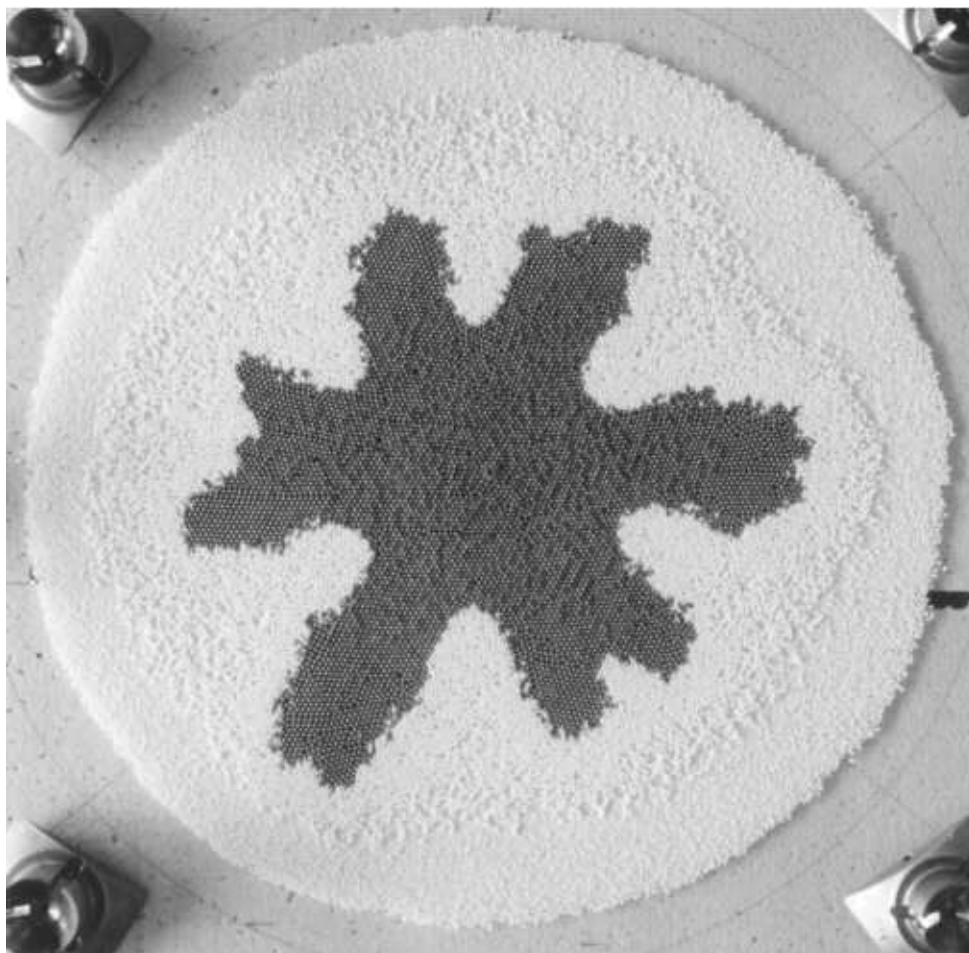


Figure 1: Fingered pattern formed by the injection of steel spheres in a monolayer of styrofoam spheres of type *B*. The plates separation is  $4.93 \pm 0.04$  mm.

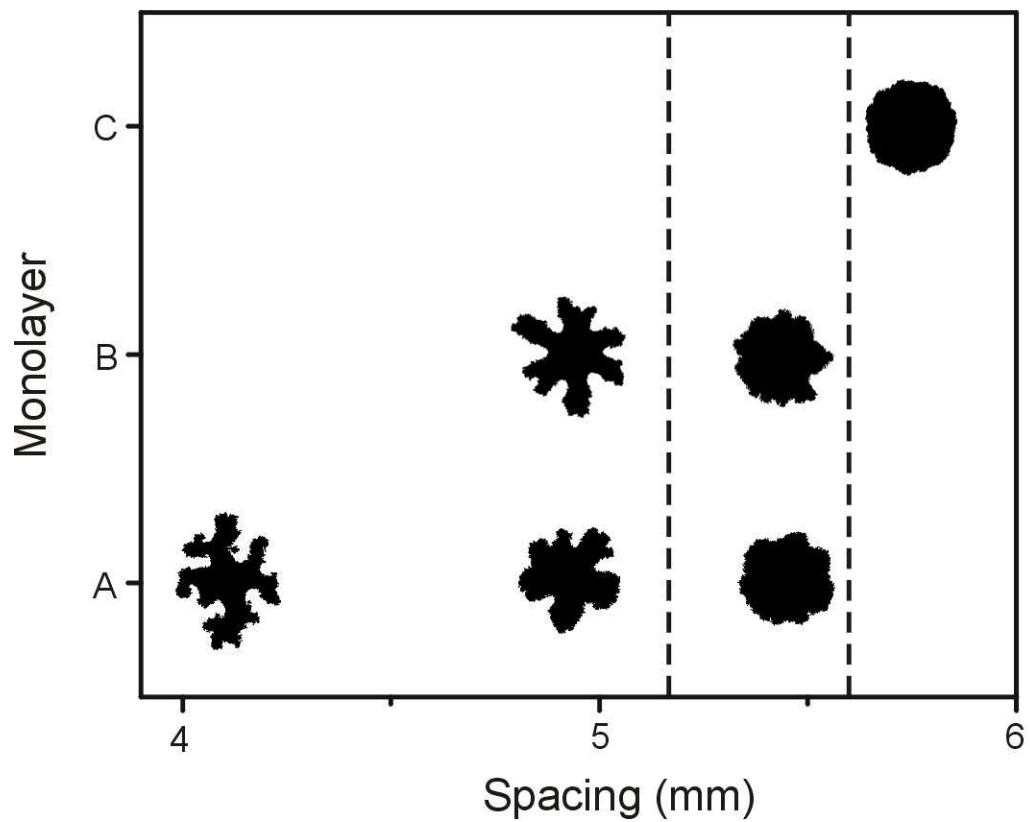


Figure 2: Morphological diagram for the patterns formed by the steel spheres injected in styrofoam particles as a function of the diameter of the styrofoam spheres and the plates separation.

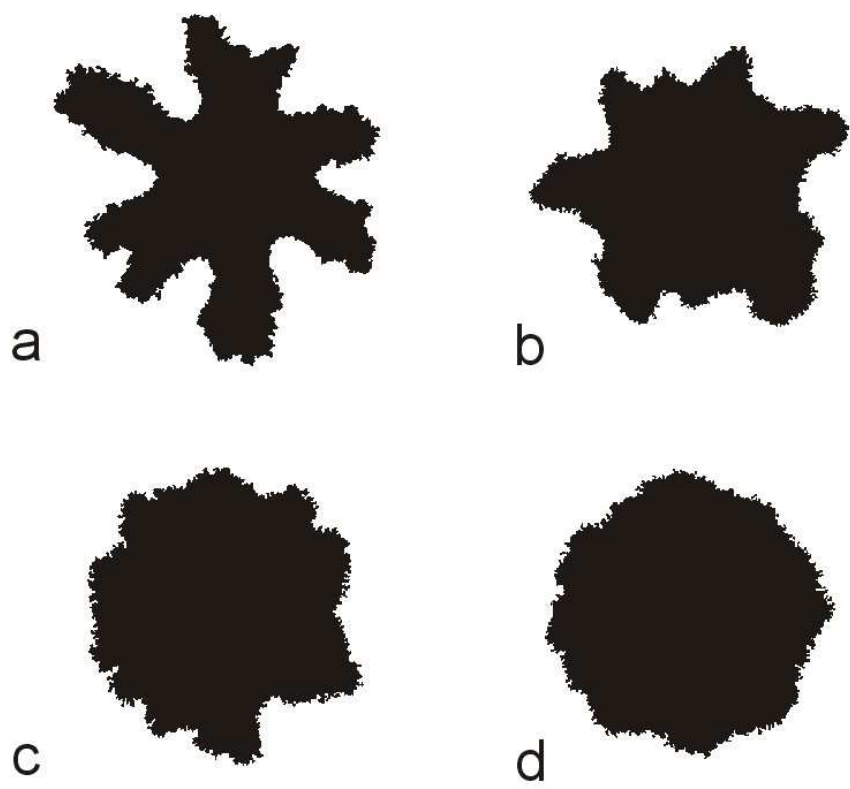


Figure 3: Morphological patterns formed by the steel spheres. The plates separation  $D$  are 4.93 mm (a), 5.17 mm (b), 5.44 (c) and 5.73 mm (d). The initial monolayer is of type  $B$ .

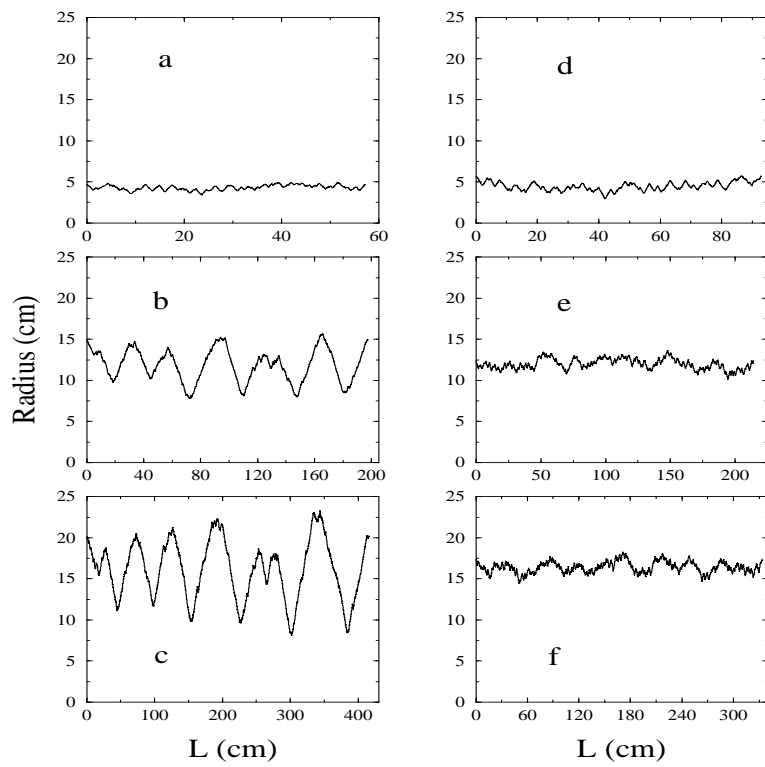


Figure 4: The border of the patterns shown in Fig. 3a (**a-c**) and Fig. 3d (**d-f**) for three different numbers of injected grains. **a,d**,  $N = 395$ . **b,e**,  $N = 3160$ . **c,f**,  $N = 5925$ .

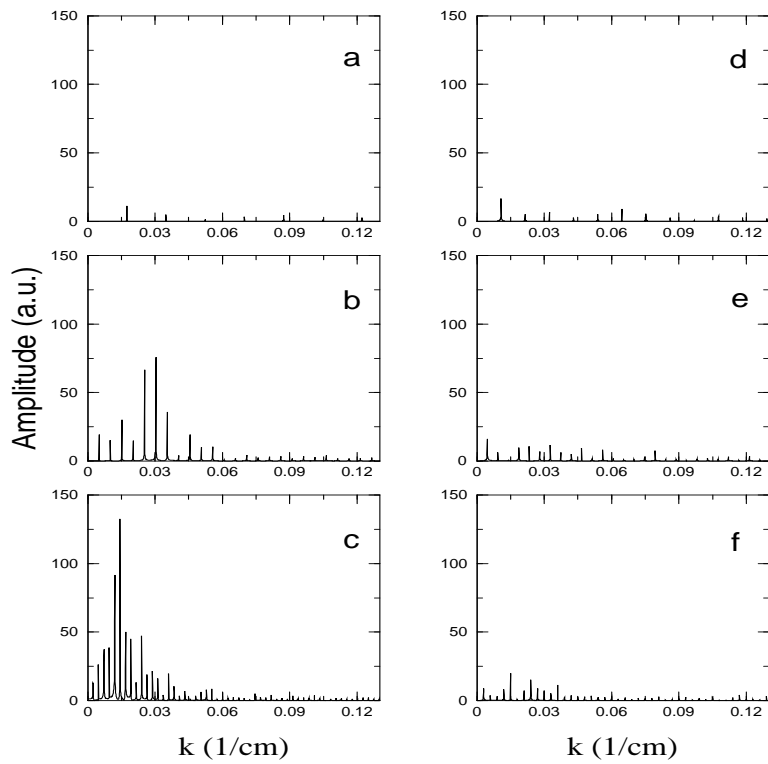


Figure 5: Power spectra of the border of the patterns shown in Fig. 4. **a-c**, Transforms for Fig. 4a-c. The two strongest modes selected correspond to the formation of fingers and their tip splitting. **d-f**, Transforms for Fig. 4d-f.